Ground and excited states of doubly open-shell nuclei from ab initio valence-space Hamiltonians

S. R. Stroberg, H. Hergert, J. D. Holt, S. K. Bogner, and A. Schwenk

Phys. Rev. C **93**, 051301 — Published 6 May 2016

DOI: 10.1103/PhysRevC.93.051301

Ground and excited states of doubly open-shell nuclei from ab initio valence-space Hamiltonians

S. R. Stroberg,[1, *] H. Hergert,[2, †] J. D. Holt,[1, ‡] S. K. Bogner,[2, §] and A. Schwenk[3, 4, ¶]

[1] *TRIUMF, 4004 Wesbrook Mall, Vancouver, British Columbia, V6T 2A3 Canada*
[2] *National Superconducting Cyclotron Laboratory and Department of Physics and Astronomy, Michigan State University, East Lansing, MI 48824, USA*
[3] *Institut für Kernphysik, Technische Universität Darmstadt, 64289 Darmstadt, Germany*
[4] *ExtreMe Matter Institute EMMI, GSI Helmholtzzentrum für Schwerionenforschung GmbH, 64291 Darmstadt, Germany*

We present ab initio predictions for ground and excited states of doubly open-shell fluorine and neon isotopes based on chiral two- and three-nucleon interactions. We use the in-medium similarity renormalization group, to derive mass-dependent *sd* valence-space Hamiltonians. The experimental ground-state energies are reproduced through neutron number $N = 14$, beyond which a new targeted normal-ordering procedure improves agreement with data and large-space multi-reference calculations. For spectroscopy, we focus on neutron-rich $^{23-26}$F and $^{24-26}$Ne isotopes near $N = 14, 16$ magic numbers. In all cases we find agreement with experiment and established phenomenology. Moreover, yrast states are well described in ^{20}Ne and ^{24}Mg, providing a path towards an ab initio description of deformation in the medium-mass region.

PACS numbers: 21.30.Fe, 21.60.Cs, 21.60.De, 21.10.-k

With hundreds of undiscovered nuclei to be created and studied at rare-isotope beam facilities, the development of an ab initio picture of exotic nuclei is a central goal of modern nuclear theory. Three-nucleon (3N) forces are a key input to understand and predict the structure of medium-mass nuclei, from the neutron dripline in oxygen to the evolution of magic numbers in oxygen and calcium [1–11]. In addition, advances in large-space many-body methods have extended the scope of ab initio theory to open-shell calcium and nickel isotopes, and beyond [12–14]. While ground-state properties of even-even isotopes are captured with these methods, excited states and/or odd-mass systems away from closed shells are more challenging. Furthermore, doubly open-shell nuclei may exhibit deformation, which is challenging to capture in large-space ab initio methods built on spherical reference states [15, 16].

These difficulties can be addressed straightforwardly within the framework of the nuclear shell model [17–19], where an effective valence-space Hamiltonian is constructed for particles occupying a small singe-particle space above some closed-shell configuration. Exact diagonalization then accesses all nuclei and their structure properties in a given region and naturally captures deformation [20]. While the shell model approach is traditionally phenomenological, valence-space Hamiltonians obtained with many-body perturbation theory (MBPT) [21] including 3N forces describe separation energies and first-excited 2^+ energies in the *sd* shell above ^{16}O [22, 23]. However, order-by-order convergence of is difficult to verify, especially for $T = 0$ components, and a successful description of exotic nuclei requires the use of extended valence spaces [24–27]. All-order diagrammatic extensions provide further insights [28] but exhibit dependence on the harmonic-oscillator spacing $\hbar\omega$ and have not been benchmarked with 3N forces. Recently, nonperturbative methods have been developed [29–33], which provide a promising path toward an ab initio description of nuclei between semi-magic isotopic chains, but have not been applied systematically beyond oxygen.

In this article we present ab initio predictions for ground and excited states in doubly open-shell nuclei using valence-space Hamiltonians derived from the in-medium similarity renormalization group (IM-SRG). Focusing on fluorine and neon isotopes within the *sd*-shell, we find that including chiral 3N forces leads to a good agreement with experimental data and state-of-the-art phenomenology [35]. We also introduce a novel targeted normal-ordering procedure, which further improves ground-state energies in comparison to experiment and large-space multi-reference IM-SRG calculations performed directly in the target nucleus. Finally we demonstrate that nuclear deformation in medium-mass nuclei emerges ab initio by studying yrast states in ^{20}Ne and ^{24}Mg and comparing with spherical ground states obtained with multi-reference IM-SRG [6].

In the IM-SRG, we start from an A-body Hamiltonian that is normal ordered with respect to a finite-A reference, e.g., a Hartree-Fock ground state, and apply a continuous unitary transformation $U(s)$ to drive the Hamiltonian to band- or block-diagonal form. In practice, this is accomplished by solving the flow equation

$$\frac{dH(s)}{ds} = [\eta(s), H(s)] , \tag{1}$$

where $U(s)$ is defined implicitly through the anti-Hermitian generator $\eta(s) \equiv [dU(s)/ds]\, U^\dagger(s)$. With a

* E-mail: sstroberg@triumf.ca
† E-mail: hergert@nscl.msu.edu
‡ E-mail: jholt@triumf.ca
§ E-mail: bogner@nscl.msu.edu
¶ E-mail: schwenk@physik.tu-darmstadt.de

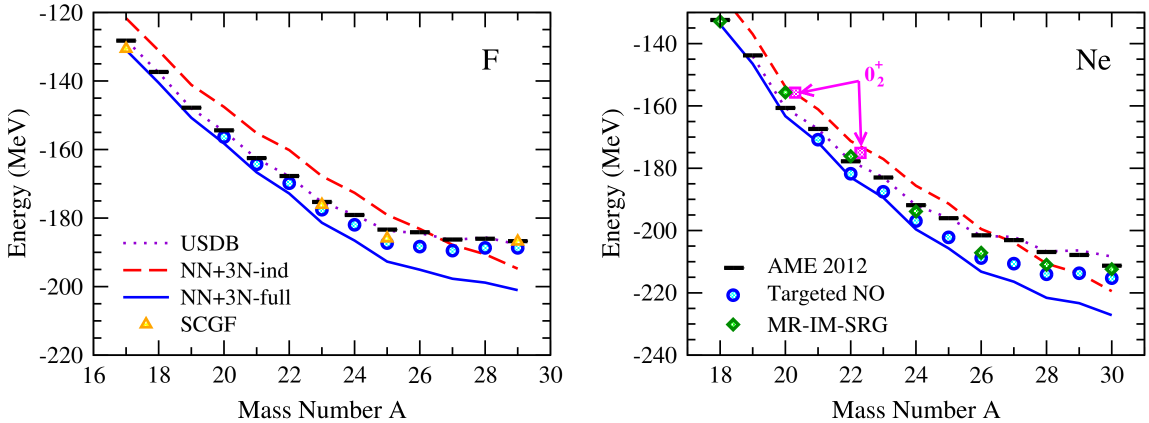

FIG. 1. Ground-state energies of fluorine and neon isotopes from the A-dependent IM-SRG valence-space Hamiltonian with $\lambda_{\rm SRG} = 1.88\,{\rm fm}^{-1}$ and $\hbar\omega = 24\,{\rm MeV}$ compared with the 2012 Atomic Mass Evaluation (AME2012) [34] and the phenomenological USDB interaction [35]. Blue circles indicate results obtained with the new targeted normal ordering (Targeted NO) scheme, yellow triangles self-consistent Green's function (SCGF) [4], and green diamonds indicate ground-state energies calculated with the multi reference (MR-IM-SRG).

suitable choice of $\eta(s)$, the off-diagonal part of the Hamiltonian, $H^{\rm od}(s)$, is driven to zero as $s \to \infty$. The freedom in defining $H^{\rm od}(s)$ allows us to tailor the decoupling to the problem of interest, e.g., the core [5, 36] or the core and a valence-space Hamiltonian [29, 30]. Within the IM-SRG(2) approximation, Eq. (1) is truncated to normal-ordered two-body operators. In the present work, we use a version of White's generator which is less susceptible to the effects of small energy denominators than the one we used in earlier work [29, 30]. Denoting generic energy denominators by Δ, $\eta = 1/2 \tan^{-1}(2H^{\rm od}/\Delta)$ [37]. We also apply the newly developed Magnus formulation [38] to decouple valence-space Hamiltonians, where the unitary transformation $U(s)$ is explicitly calculated, making the calculation of general effective operators for observables such as radii or electroweak transitions tractable. Results calculated within both frameworks agree at the 10 keV level for both core and valence-space decoupling.

To implement the IM-SRG, we start from the $\Lambda_{\rm NN} =$ 500 MeV chiral $\rm N^3LO$ NN interaction of Refs. [39, 40] and evolve with the free-space SRG [41, 42] to low-momentum resolution scales, $\lambda_{\rm SRG} = 1.88-2.11\,{\rm fm}^{-1}$. The NN+3N-induced (NN+3N-ind) Hamiltonians includes 3N forces induced by the evolution and correspond to the original NN interaction, up to neglected induced four- and higher-body forces [42, 43]. The NN+3N-full Hamiltonians include an initial local $\Lambda_{\rm 3N} = 400\,{\rm MeV}$ chiral $\rm N^2LO$ 3N interaction [44], consistently evolved to $\lambda_{\rm SRG}$. This value of $\Lambda_{\rm 3N}$ minimizes the effects of induced 4N interactions in the region of oxygen [30, 45, 46]. Calculations in oxygen isotopes with $\Lambda_{\rm 3N} = 500\,{\rm MeV}$ displayed a pronounced sensitivity to $\lambda_{\rm SRG}$ [30], making it difficult to disentangle uncertainties originating from neglected induced forces and the initial Hamiltonian. To obtain the final input Hamiltonian, we add the A-dependent intrinsic kinetic energy. Here, we choose A to be the mass of the target nucleus, for which we wish to approximate an exact no-core diagonalization. An A-independent prescription introduces an error that grows with the number of valence nucleons [47].

We then solve the Hartree-Fock equations to obtain the core reference state. We normal order the Hamiltonian with respect to the Hartree-Fock reference state and discard residual three-body forces [48]. The normal-ordered 0-, 1-, and 2-body parts are taken as initial values in the IM-SRG decoupling within a single-particle basis $e = 2n + l \leq e_{\rm max} = 14$, with an additional cut $e_1 + e_2 + e_3 \leq E_{\rm 3max} = 14$ for 3N forces [46].

The IM-SRG is used to decouple the core and valence space from excitations, and the core energy, valence-space single-particle energies, and two-body matrix elements are taken from the evolved $s \to \infty$ Hamiltonian [29, 30]. We work within the standard sd shell consisting of the proton and neutron $d_{5/2}$, $d_{3/2}$, and $s_{1/2}$ orbits above the ^{16}O core. We diagonalize the A-dependent valence-space Hamiltonian to obtain ground-state energies and natural-parity spectra using the NushellX and Oslo shell model codes [49, 50]. Since it is well known that the NN+3N-full initial Hamiltonian used in these calculations produces systematic overbinding and too-small radii in calcium [12–14], we limit our discussion to isotopic chains in the lower sd shell, in particular fluorine and neon, which serve to test proton-proton, neutron-neutron, and proton-neutron valence-space matrix elements. With increasing valence particle number, ab initio valence-space Hamiltonians must also systematically account for 3N forces within the valence space, an issue we address when discussing our targeted normal ordering approach.

We first consider ground-state energies in fluorine and neon isotopes, which have been explored with self-consistent Green's function calculations for particular isotopes [4, 52] and valence-space Hamiltonians from MBPT [1, 23]. IM-SRG results through $N = 20$ are shown in Fig. 1, compared with experiment and phe-

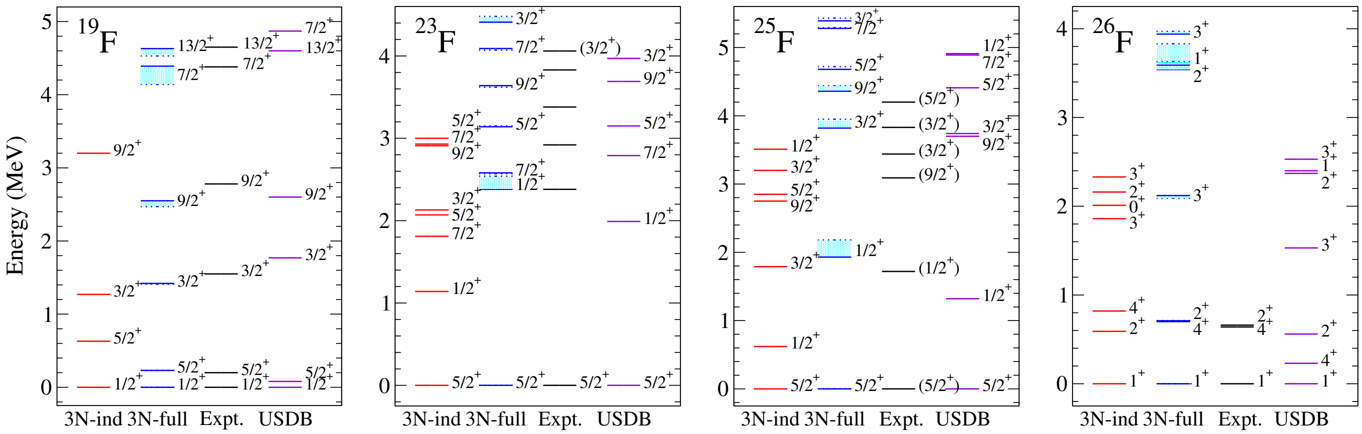

FIG. 2. Excited-state spectra for ^{19,23,25,26}F from IM-SRG Hamiltonians based on NN+3N-ind and NN+3N-full Hamiltonians for $\Lambda_{3\mathrm{N}} = 400\,\mathrm{MeV}$ with $\hbar\omega = 20\,\mathrm{MeV}$ (dotted) and $\hbar\omega = 24\,\mathrm{MeV}$ (solid), compared with experiment [51] and results from the phenomenological USDB interaction [35].

nomenological USDB predictions [35]. Since core properties are calculated consistently in our IM-SRG framework, we quote absolute ground-state energies in all calculations, but normalize USDB results to the experimental ground state of ^{16}O. We first observe that NN+3N-ind Hamiltonians exhibit incorrect trends throughout both isotopic chains, reminiscent of the incorrect dripline predictions in oxygen isotopes [1, 2, 30]. With NN+3N-full Hamiltonians, the agreement is improved, including the flattening of energies in the neutron-rich region. We note a very minor $\hbar\omega$ dependence of ground-state energies for $\hbar\omega = 20-24\,\mathrm{MeV}$, not shown in Fig. 1. The largest deviations are 600 keV in ^{29}F and 1.3 MeV in ^{30}Ne, a 0.5% effect, indicating good convergence with respect to the model space truncation.

It is apparent, however, that near $N = 14$, NN+3N-full results become overbound with respect to experiment, similar to oxygen isotopes [30]. We also plot in Fig. 1 multi-reference IM-SRG calculations of ground-state energies in even neon isotopes based on the same initial Hamiltonian, which display an improved agreement with experiment outside of ^{20,22}Ne. One obvious difference between the valence-space and multi-reference formulations is that the latter is carried out in the target nucleus. In the valence-space calculations, the Hamiltonian is instead normal ordered with respect to the ^{16}O core, which neglects 3N forces between valence nucleons. This approximation works well for few valence nucleons, but residual 3N effects scale as A_v/A_c [53] for normal Fermi systems, and therefore cannot be neglected as the number of valence nucleons increases [25, 54].

To mitigate this effect, we introduce a targeted normal ordering approach in which the normal ordering is first performed with respect to the nearest closed shell rather than the ^{16}O core. We then apply the IM-SRG to decouple the ^{16}O core and *sd* valence space. Finally, we re-normal order with respect to ^{16}O to perform a full *sd*-shell diagonalization. The results of this procedure are shown in both figures, which provides 12 MeV additional repulsion at $N = 20$ and improves agreement with experiment. More importantly, there are only modest differences between the shell model results and large-space self-consistent Green's function and multi-reference IM-SRG calculations in fluorine and neon, respectively. Furthermore the impact on spectra is generally minor for both isotopic chains.

For spectroscopy in the fluorine and neon isotopes, we highlight the $N = 14, 16$ region towards the experimental limits, in addition to one example at stability, though for completeness, we show spectra for all F, Ne, Na, and Mg isotopes within the *sd* shell as supplementary material [55]. The only ab initio predictions in fluorine are large-scale coupled-cluster calculations in ^{26}F using a phenomenological 3N force [56] and ^{22,24}F using optimized chiral interactions at order N^{2}LO [57]. In both cases, spectra are reasonable, but the density and ordering of states can deviate from experiment [1, 57]. IM-SRG calculations in ^{24}F succeeded in predicting properties of newly measured states [58]. There are no ab initio predictions for spectra in neon except for the first excited 2^+ energies in even isotopes from MBPT shell model based on 3N forces [23]. Finally, we denote the $\hbar\omega$ dependence of spectra with shaded bands in NN+3N-full results. While often at the 100 keV level or less, in a few cases it approaches 400 keV.

In Fig. 2 we show the calculated spectra of ^{19,23,25,26}F. We first observe that in all cases, NN+3N-ind forces give too-compressed spectra with an incorrect ordering of levels, even in the stable ^{19}F. With initial 3N forces, the spectra are clearly improved. The spectrum of ^{19}F agrees very well with experiment, even giving the correct $7/2^+$–$13/2^+$ ordering not reproduced by USDB. For the neutron-rich isotopes, experimental data are fewer. Nonetheless the spacing of the mostly unidentified levels in ^{23}F are reproduced, and spin-parity assignments agree with USDB below 4 MeV. In ^{25}F neither IM-SRG

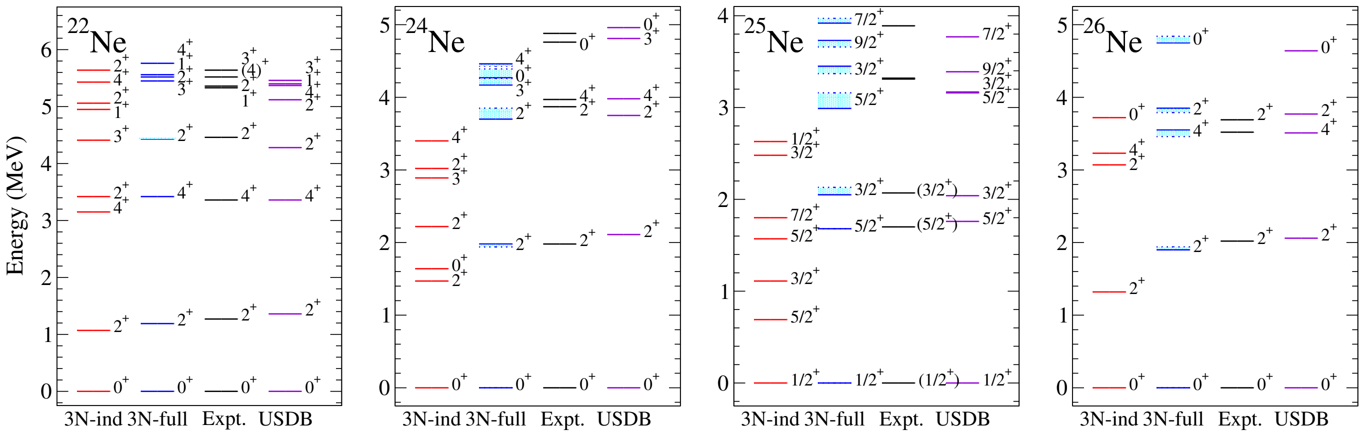

FIG. 3. Excited-state spectra of ^{19,24,25,26}Ne, as in Fig. 2.

nor USDB fully predict the experimental spectrum and, despite similar spacings, do not agree on the ordering of states. Finally in ^{26}F only the lowest excited states are known and are well reproduced by IM-SRG. The ordering of higher-lying excited states agrees well with USDB, but the increased energy is likely due to a lack of continuum effects, which are implicitly included in the phenomenology. Additional experimental spin/parity assignments are needed to conclusively test our predictions.

In Fig. 3 we show calculations for the stable ^{22}Ne and exotic $^{24-26}$Ne nuclei. Experimental data are limited, but in all cases, spectra without initial 3N forces are too compressed with respect to experiment, particularly ^{25}Ne. With initial 3N forces, the spectra are improved throughout the chain. For example in ^{25,26}Ne the ordering of states is in complete agreement with USDB, strongly suggesting the unidentified excited state in ^{26}Ne as a 4^+, but more experimental data are needed.

While predictions for individual nuclei in the lower *sd* shell can be seen in the supplementary material [55], it may be difficult to conclude definitively on the quality of these predictions with respect to experiment and USDB. Therefore we have calculated the root-mean-squared deviation from 144 experimental levels in the *sd*-shell $Z = 8 - 12$ isotopes. For the shell model IM-SRG (USDB) interactions, we find values of 513(244) keV in oxygen, 446(200) keV in fluorine, 388(268) keV in neon, 572(155) keV in sodium, and 791(106) keV in magnesium. While the experimental agreement for fluorine and neon is an improvement over the description of oxygen isotopes in Ref. [30], the decreased accuracy for magnesium in particular is likely due to a combination of neglected 3N forces between valence-space nucleons and a deterioration of the NN+3N-full Hamiltonians.

Finally we turn to deformation, which can be treated ab initio in light nuclei with Green's Function Monte Carlo [59], with the standard or symplectic no-core shell model [60–62], and with lattice EFT [63], or within an EFT framework for heavy nuclei [64, 65]. Deformation is challenging for ab initio methods to capture in

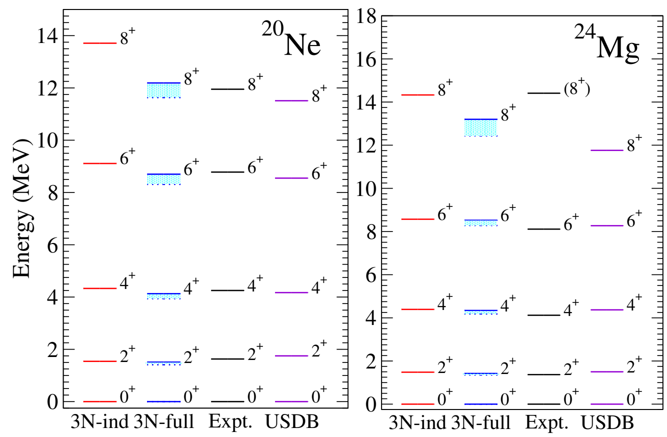

FIG. 4. Yrast states for deformed ^{20}Ne and ^{24}Mg compared to experimental data and phenomenological USDB predictions.

medium-mass nuclei, where spherical symmetry is typically assumed, and extensions to the computationally demanding *m*-scheme are required for a proper treatment. Within the present framework, deformation can emerge naturally from valence-space configuration mixing, and here we investigate the extent to which this is realized. One key signature of deformation is the presence of a rotational spectrum. ^{20}Ne and ^{24}Mg provide classic examples of rotational spectra in the lower *sd* shell, and these spectra are well reproduced in all calculations, as shown in Fig. 4, though somewhat improved with the inclusion of 3N forces. Further evidence of deformation may be deduced from Fig. 1, where we note a significant discrepancy in the ^{20,22}Ne ground-state energies obtained with the shell model and multi-reference calculations. This may be understood by considering that the multi-reference IM-SRG, which is built on *intrinsically spherical* reference states, cannot produce a deformed ground state. We might expect that instead it selects the lowest-energy state with spherical intrinsic structure, and indeed, we find that the energy of the first excited 0^+ state from the valence space calculation aligns remarkably well with the multi-reference result in Fig. 1.

In conclusion, we have presented ab initio calculations for doubly open-shell nuclei from A-dependent IM-SRG valence-space Hamiltonians. With initial 3N forces, excited states are in agreement with experiment, and with a new targeted normal ordering procedure, ground-state energies are improved with respect to experiment and large-space multi-reference IM-SRG calculations. A systematic application of targeted normal ordering, which better accounts for effects of 3N forces between valence space particles, will allow ab initio calculations throughout the *sd* shell. Comparison with multi-reference IM-SRG indicates that the valence-space IM-SRG calculations produce deformed ground states in ^{20,22}Ne and predict rotational yrast states in deformed ^{20}Ne and ^{24}Mg, illustrating that deformation can be captured in this ab initio framework. To further explore deformation in the *sd* shell, the Magnus formulation allows straightforward evaluation of relevant effective valence-space operators such as quadrupole moments and $E2$ transitions, and ultimately extensions to other operators will allow ab initio predictions for important electroweak processes such as neutrinoless double-beta decay [66–68].

a. Acknowledgments. We thank A. Calci, J. Menéndez, T. Morris, P. Navrátil, N. Parzuchowski, A. Poves, J. Simonis, and O. Sorlin for useful discussions and S. Binder, A. Calci, J. Langhammer, and R. Roth for the SRG-evolved NN+3N matrix elements. TRIUMF receives funding via a contribution through the National Research Council Canada. This work was supported in part by NSERC, the NUCLEI SciDAC Collaboration under the U.S. Department of Energy Grants No. DE-SC0008533 and DE-SC0008511, the National Science Foundation under Grants No. PHY-1404159, the European Research Council Grant No. 307986 STRONGINT, and the BMBF under Contracts No. 06DA70471 and 05P15RDFN1. Computations were performed with an allocation of computing resources at the Jülich Supercomputing Center, Ohio Supercomputer Center (OSC), and the Michigan State University High Performance Computing Center (HPCC)/Institute for Cyber-Enabled Research (iCER).

b. Note added. Very recently Jansen et al. [69] applied the complementary coupled-cluster effective-interaction method to construct A-independent nonperturbative shell-model interactions also to explore deformation in the *sd* shell.

[1] K. Hebeler, J. D. Holt, J. Menéndez, and A. Schwenk, Ann. Rev. Nucl. Part. Sci. **65**, 457 (2015).
[2] T. Otsuka, T. Suzuki, J. D. Holt, A. Schwenk, and Y. Akaishi, Phys. Rev. Lett. **105**, 032501 (2010).
[3] G. Hagen, M. Hjorth-Jensen, G. R. Jansen, R. Machleidt, and T. Papenbrock, Phys. Rev. Lett. **108**, 242501 (2012).
[4] A. Cipollone, C. Barbieri, and P. Navrátil, Phys. Rev. Lett. **111**, 062501 (2013).
[5] H. Hergert, S. K. Bogner, S. Binder, A. Calci, J. Langhammer, and A. Schwenk, Phys. Rev. C **87**, 034307 (2013).
[6] H. Hergert, S. Binder, A. Calci, J. Langhammer, and R. Roth, Phys. Rev. Lett. **110**, 242501 (2013).
[7] J. D. Holt, T. Otsuka, A. Schwenk, and T. Suzuki, J. Phys. G **39**, 085111 (2012).
[8] G. Hagen, M. Hjorth-Jensen, G. R. Jansen, R. Machleidt, and T. Papenbrock, Phys. Rev. Lett. **109**, 032502 (2012).
[9] A. T. Gallant *et al.*, Phys. Rev. Lett. **109**, 032506 (2012).
[10] F. Wienholtz *et al.*, Nature **498**, 346 (2013).
[11] J. D. Holt, J. Menéndez, and A. Schwenk, Phys. Rev. Lett. **110**, 022502 (2013).
[12] V. Somà, A. Cipollone, C. Barbieri, P. Navrátil, and T. Duguet, Phys. Rev. C **89**, 061301(R) (2014).
[13] S. Binder, J. Langhammer, A. Calci, and R. Roth, Phys. Lett. B **736**, 119 (2014).
[14] H. Hergert, S. K. Bogner, T. D. Morris, S. Binder, A. Calci, J. Langhammer, and R. Roth, Phys. Rev. C **90**, 041302(R) (2014).
[15] A. Signoracci, T. Duguet, G. Hagen, and G. R. Jansen, Phys. Rev. C **91**, 064320 (2015).
[16] T. Duguet, J. Phys. G **42**, 025107 (2015).
[17] B. A. Brown, Prog. Part. Nucl. Phys. **47**, 517 (2001).
[18] E. Caurier, G. Martinez-Pinedo, F. Nowacki, A. Poves, and A. P. Zuker, Rev. Mod. Phys. **77**, 427 (2005).
[19] T. Otsuka, Phys. Scripta **T152**, 014007 (2013).
[20] J. P. Elliot, Proc. R. Soc. London **245**, 128 (1958).
[21] M. Hjorth-Jensen, T. T. S. Kuo, and E. Osnes, Phys. Rept. **261**, 125 (1995).
[22] A. T. Gallant *et al.*, Phys. Rev. Lett. **113**, 082501 (2014).
[23] J. Simonis, K. Hebeler, J. D. Holt, J. Menéndez, and A. Schwenk, Phys. Rev. C **93**, 011302 (2016).
[24] J. D. Holt, J. Menéndez, and A. Schwenk, Eur. Phys. J. A **49**, 39 (2013).
[25] J. D. Holt, J. Menéndez, J. Simonis, and A. Schwenk, Phys. Rev. C **90**, 024312 (2014).
[26] N. Tsunoda, K. Takayanagi, M. Hjorth-Jensen, and T. Otsuka, Phys. Rev. C **89**, 024313 (2014).
[27] H. Dong, T. T. S. Kuo, and J. W. Holt, Nucl. Phys. **A930**, 1 (2014).
[28] J. D. Holt, J. W. Holt, T. T. S. Kuo, G. E. Brown, and S. K. Bogner, Phys. Rev. C **72**, 041304 (2005).
[29] K. Tsukiyama, S. K. Bogner, and A. Schwenk, Phys. Rev. C **85**, 061304(R) (2012).
[30] S. K. Bogner, H. Hergert, J. D. Holt, A. Schwenk, S. Binder, A. Calci, J. Langhammer, and R. Roth, Phys. Rev. Lett. **113**, 142501 (2014).
[31] G. R. Jansen, J. Engel, G. Hagen, P. Navrátil, and A. Signoracci, Phys. Rev. Lett. **113**, 142502 (2014).
[32] A. F. Lisetskiy, B. R. Barrett, M. K. G. Kruse, P. Navrátil, I. Stetcu, and J. P. Vary, Phys. Rev. C **78**, 044302 (2008).
[33] E. Dikmen, A. F. Lisetski, B. R. Barrett, P. Maris, A. M. Shirokov, and J. P. Vary, Phys. Rev. C **91**, 064301 (2015).

[34] M. Wang, G. Audi, A. H. Wapstra, F. G. Kondev, M. MacCormick, X. Xu, and B. Pfeiffer, Chin. Phys. C **36**, 1603 (2012).
[35] B. A. Brown and W. A. Richter, Phys. Rev. C **74**, 034315 (2006).
[36] K. Tsukiyama, S. K. Bogner, and A. Schwenk, Phys. Rev. Lett. **106**, 222502 (2011).
[37] S. R. White, J. Chem. Phys **117**, 7472 (2002).
[38] T. D. Morris, N. Parzuchowski, and S. K. Bogner, Phys. Rev. C **92**, 034331 (2015).
[39] D. R. Entem and R. Machleidt, Phys. Rev. C **68**, 041001(R) (2003).
[40] R. Machleidt and D. R. Entem, Phys. Rept. **503**, 1 (2011).
[41] S. K. Bogner, R. J. Furnstahl, and R. J. Perry, Phys. Rev. C **75**, 061001(R) (2007).
[42] S. K. Bogner, R. J. Furnstahl, and A. Schwenk, Prog. Part. Nucl. Phys. **65**, 94 (2010).
[43] E. D. Jurgenson, P. Navrátil, and R. J. Furnstahl, Phys. Rev. Lett. **103**, 082501 (2009).
[44] P. Navrátil, Few Body Syst. **41**, 117 (2007).
[45] R. Roth, S. Binder, K. Vobig, A. Calci, J. Langhammer, and P. Navrátil, Phys. Rev. Lett. **109**, 052501 (2012).
[46] R. Roth, A. Calci, J. Langhammer, and S. Binder, Phys. Rev. C **90**, 024325 (2014).
[47] S. R. Stroberg *et al.*, in preparation.
[48] G. Hagen, T. Papenbrock, D. J. Dean, A. Schwenk, A. Nogga, M. Wloch, and P. Piecuch, Phys. Rev. C **76**, 034302 (2007).
[49] B. A. Brown and W. D. M. Rae, Nucl. Data Sheets **120**, 115 (2014).
[50] T. Engeland and M. Hjorth-Jensen, Oslo-FCI code https://github.com/ManyBodyPhysics/ManybodyCodes/.
[51] http://www.nndc.bnl.gov/ensdf/.
[52] A. Cipollone, C. Barbieri, and P. Navrátil, Phys. Rev. C **92**, 014306 (2015).
[53] B. Friman and A. Schwenk, In *From Nuclei to Stars: Festschrift in Honor of Gerald E. Brown*, ed. S. Lee, p. 141. Singapore: World Scientific (2011).
[54] C. Caesar *et al.* (R3B collaboration), Phys. Rev. C **88**, 034313 (2013).
[55] See Supplemental Material at [URL will be inserted by publisher] for spectra for all F, Ne, Na, and Mg isotopes within the *sd* shell.
[56] A. Lepailleur *et al.*, Phys. Rev. Lett. **110**, 082502 (2013).
[57] A. Ekström, G. R. Jansen, K. A. Wendt, G. Hagen, T. Papenbrock, S. Bacca, B. Carlsson, and D. Gazit, Phys. Rev. Lett. **113**, 262504 (2014).
[58] L. Cáceres *et al.*, Phys. Rev. C **92**, 014327 (2015).
[59] S. C. Pieper, R. B. Wiringa, and J. Carlson, Phys. Rev. C **70**, 054325 (2004).
[60] E. Caurier, P. Navrátil, W. E. Ormand, and J. P. Vary, Phys. Rev. C **64**, 051301 (2001).
[61] T. Dytrych, K. D. Launey, J. P. Draayer, P. Maris, J. P. Vary, E. Saule, U. Catalyurek, M. Sosonkina, D. Langr, and M. A. Caprio, Phys. Rev. Lett. **111**, 252501 (2013).
[62] M. A. Caprio, P. Maris, J. P. Vary, and R. Smith, Int. J. Mod. Phys. E **24**, 1541002 (2015).
[63] T. A. Lähde, E. Epelbaum, H. Krebs, D. Lee, U.-G. Meißner, and G. Rupak, Phys. Lett. B **732**, 110 (2014).
[64] T. Papenbrock, Nucl. Phys. A **852**, 36 (2011).
[65] E. A. Coello Pérez and T. Papenbrock, Phys. Rev. C **92**, 014323 (2015).
[66] F. T. Avignone III, S. R. Elliott, and J. Engel, Rev. Mod. Phys. **80**, 481 (2008).
[67] J. Menéndez, D. Gazit, and A. Schwenk, Phys. Rev. Lett. **107**, 062501 (2011).
[68] J. D. Holt and J. Engel, Phys. Rev. C **87**, 064315 (2013).
[69] G. R. Jansen, A. Signoracci, G. Hagen, and P. Navrátil, arXiv:1511.00757.